

Focusing and diffraction effects in angle-resolved x-ray photoelectron spectroscopy

H. C. Poon and S. Y. Tong*

Laboratory for Surface Studies and Department of Physics,
University of Wisconsin-Milwaukee, Milwaukee, Wisconsin 53201

(Received 15 August 1984)

We have analyzed angle-resolved x-ray photoelectron spectroscopy data and found that large intensity enhancements along internuclear axes are due to forward-direction focusing of the electron beam by an attractive potential. Away from the internuclear axes, we found secondary peaks whose intensity is dominated by a structure factor. Results of forward-direction focusing for Cu(001) are presented and a high-energy limit of the internuclear enhancement is derived.

Recent experimental data by Egelhoff¹ show large variations in the intensities of angle-resolved x-ray photoelectron spectroscopy (XPS) and Auger-electron spectroscopy (AES) as a function of the emission angle. Some peaks coincide with the directions of internuclear axes of the emission site and its neighbors. Other peaks, however, are not related to such directions.

We have analyzed this phenomenon and found that the measured peaks are due to two different physical processes. The first is an intensity enhancement in the forward direction due to focusing of a high-energy electron beam by an attractive (Coulomb) potential. This forward-direction focusing (FDF) effect produces an enhancement whose value approaches a limit as the kinetic energy (E_k) of the photoelectron approaches infinity. The second process governs the intensity at directions away from the internuclear axes. At these other directions, the intensity is dominated by a structure factor.

Our analysis shows that in the high-energy regime, there is always a peak in the intensity in the forward direction along internuclear axes. The half-width of this peak decreases as E_k of the photoelectron increases. Away from the internuclear axis, we expect secondary peaks whose (angular) position depends sensitively on E_k as well as the distance between atoms.

In angle-resolved XPS, the differential cross section can be written as²⁻⁴

$$\frac{d\sigma}{d\Omega} = \frac{2\pi\hbar^2 ck_0^{\text{out}}}{m\omega} \left| \frac{k_{\perp}^{\text{out}}}{k_{\perp}} \right|^2 e^{-2Imk_{\perp}|z_0|} \times \left| F_D(\hat{k}) + \sum_j e^{ik_0 R_j(1-\cos\theta_j)} \left(\frac{f(\theta_j) F_D(\hat{R}_j)}{R_j} \right) \right|^2, \quad (1)$$

TABLE I. Scattering factors for Cu at different energy (at $\theta=0$).

Energy (eV)	$ f(0) $ (Bohr radius)	$Re f(0)$ (Bohr radius)
20	0.3213	-0.2471
60	1.4366	1.0550
100	2.9187	1.9406
400	5.4014	3.8129
800	6.2759	4.8627
1600	7.0017	5.7749
$f_{\text{Born}}(0) = 10.4649$		

where \vec{R}_j is a vector from the emission site to the j th atom, \vec{k} the electron wave vector inside the solid in the direction of the detector, and k_{\perp} and k_0 its perpendicular component (to surface) and magnitude, respectively. The quantities \vec{k}^{out} , k_{\perp}^{out} , k_0^{out} are the corresponding values outside the solid, θ_j is the angle between \vec{k} and \vec{R}_j , and

$$F_D(\hat{R}) = \frac{2m}{\hbar^2} \sum_L Y_L(\hat{R}) M_{LL_i} / A_{\text{ph}}.$$

The quantity M_{LL_i} is the photoemission matrix element for an isolated atom³ and A_{ph} is amplitude of the vector potential. The quantity $f(\theta_j)$ is the scattering factor of the j th atom and ω is the photon frequency.

Along the internuclear direction of the j th atom, $\theta_j = 0$ and $\hat{R}_j = \hat{k}$, then the enhancement factor is $|1 + [f(0)/R_j]|^2$. A sufficient condition for the enhancement factor to be larger than 1 is $Re f(0) > 0$. For example, in the case of copper, $Re f(0)$ is positive for E_k above 40 eV; therefore, forward scattering is always enhanced above this energy. In the limit $E_k \rightarrow \infty$, we can evaluate $f(0)$ as

$$f_{\text{Born}}(0) = -\frac{2m}{\hbar^2} \int V(r) r^2 dr. \quad (2)$$

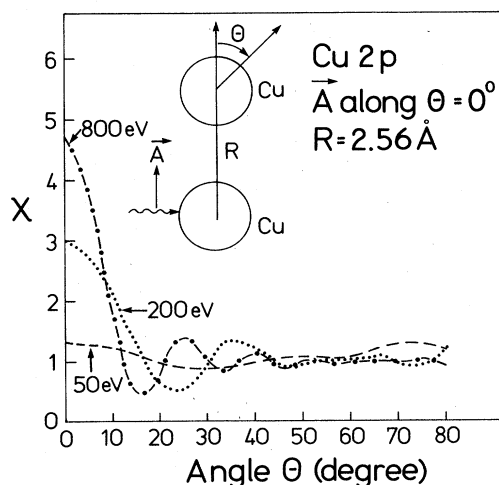


FIG. 1. The enhancement χ as a function of electron exit angle for electron energies 50, 200, and 800 eV.

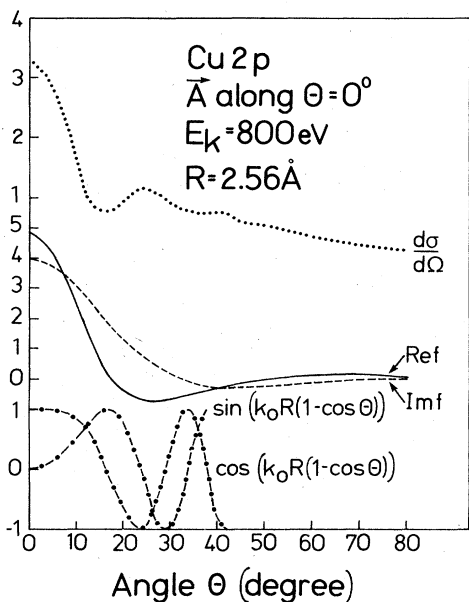


FIG. 2. Real and imaginary parts of scattering factor of Cu, real and imaginary parts of $e^{ikR(1-\cos\theta)}$ and $d\sigma/d\Omega$ (system) as a function of electron exit angle at $E_k = 800$ eV.

Since this quantity is independent of energy, it gives a high-energy limit to the enhancement factor in the forward direction. From Eq. (2), we note that $f_{\text{Born}}(0)$ is positive for a negative potential $[V(r)]$. In Table I, we tabulate $f(0)$ for Cu at a number of energies and compare it with $f_{\text{Born}}(0)$, which is only valid at very high energies.

In Fig. 1, we show the enhancement

$$\chi = \frac{d\sigma}{d\Omega} (\text{system}) / \frac{d\sigma}{d\Omega} (\text{isolated atom})$$

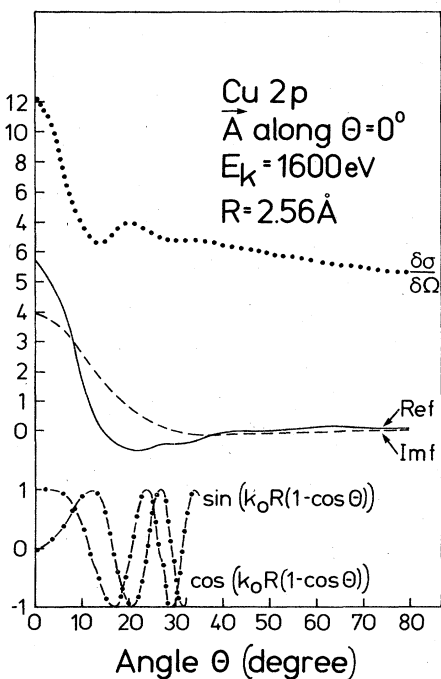


FIG. 3. Same as in Fig. 2, but $E_k = 1600$ eV.

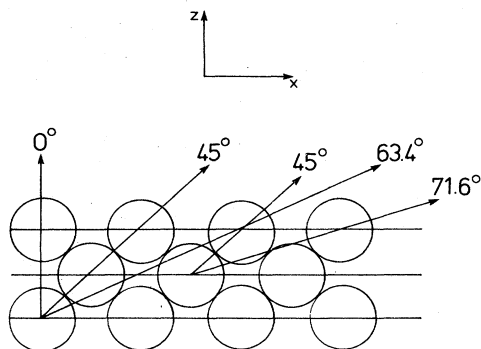


FIG. 4. Internuclear directions for 3 layers of atoms for Cu(100); the x axis is along $\langle 100 \rangle$.

for an emitting atom and a neighbor placed at a distance 2.56 \AA from it. We note that the enhancement along the forward direction increases as E_k increases, while its half-width decreases. For Cu, the enhancement approaches the limiting value of $|1 + [f_{\text{Born}}(0)/R]|^2 = 10$, using $R = 2.56 \text{ \AA}$.⁵

From Fig. 1, we see that the secondary peak moves closer to zero as E_k increases. To understand this effect, we have plotted $\text{Re}f(\theta)$ and $\text{Im}f(\theta)$, the real and imaginary parts of the structure factor $e^{ikR(1-\cos\theta)}$ for the energies 800 and 1600 eV in Figs. 2 and 3, respectively. We note that the secondary peaks are mainly caused by the structure factor which is an oscillating function of θ . The first minimum of the structure factor moves closer to the zero angle as E_k is increased. Higher-order peaks at large angles are extremely small since $f(\theta)$ approaches zero as θ increases.

We have analyzed the angle-resolved XPS intensity spectra from the Cu 2p core level for the case considered by Egelhoff,¹ i.e., 2 and 3 layers of Cu. We show in Fig. 4 the internuclear angles measured from the surface normal. Figure 5 shows the calculated curves for \vec{A} polarized parallel to the surface along the x direction. We note that the peak at 45° for both 2 and 3 layers is due to nearest-neighbor focusing effect, while the small peak at 0° (for 3 layers) is due to next neighbor focusing. The peak at 22.5° (for both 2 and 3 layers) is due to interference effects, while the broad

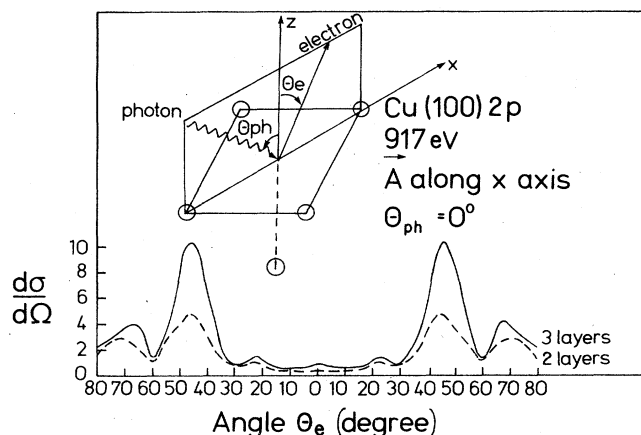


FIG. 5. Polar plot of Cu(100) 2p photoemission at 917 eV for 2 and 3 layers. \vec{A} is along x axis with $\theta_{\text{ph}} = 0^\circ$.

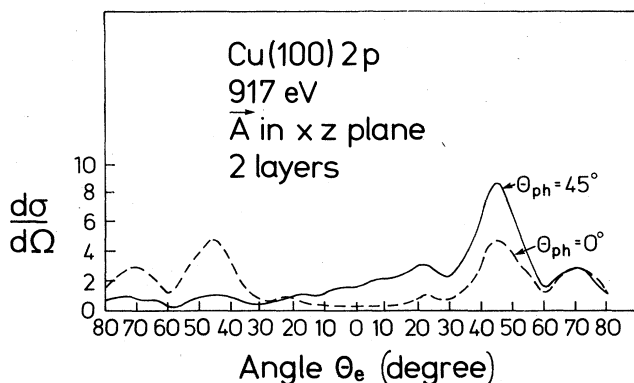


FIG. 6. Polar plot of Cu(100) 2p photoemission at 917 eV for 2 layers; \vec{A} is within the xz plane and $\theta_{ph} = 0^\circ, 45^\circ$.

peaks at 70.8° (for 2 layers) and 67.5° (for 3 layers) are due to a combination of focusing and interference effects. It is interesting to note that there is no peak at 63.4° for the 3 layer case, because the internuclear distance is large.

We can enhance the intensity peak along a certain inter-nuclear direction if we put \vec{A} along this direction. An example is shown in Fig. 6, where the \vec{A} vector is along $\theta = 45^\circ$ and we note that the peak intensity along that direction is enhanced by more than a factor of 2.

Finally, we investigate the sensitivity of the intensity peaks to structural changes. In Fig. 7, we show how $d\sigma/d\Omega$ changes as we vary the spacing between copper layers from 1.76 to 1.96 Å in steps of 0.1 Å, for the 2 layer case. The peak at $\theta = 45^\circ$ moves to $\theta = 43.4^\circ$ and 41.9° , respectively, tracking the internuclear directions. On the other hand, peaks near 22° and 70° bear no direct relation to any internuclear directions.

In summary, this analysis of the origin of intensity peaks should help the interpretation of experimental angle-resolved XPS data. Peaks whose angular positions remain *unchanged* as the photon energy is varied are related to near-neighbor internuclear directions. The angles of these peaks therefore should provide direct structural information. For example, one can use this phenomenon to study epitax-

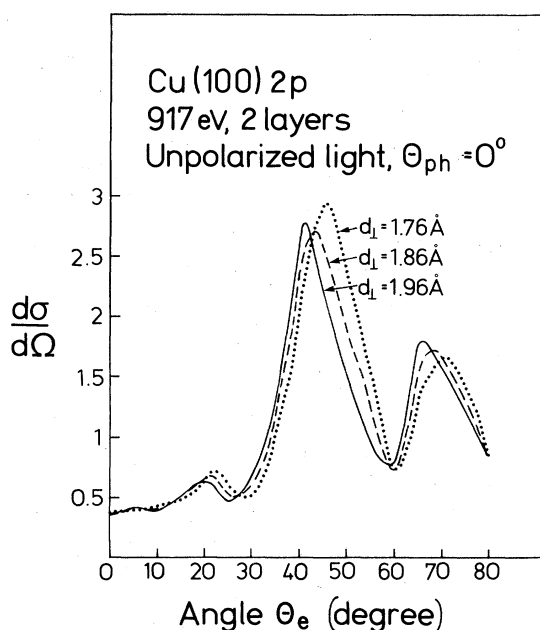


FIG. 7. Polar plot of Cu(100) 2p photoemission at 917 eV for 2 layers, unpolarized light and $\theta_{ph} = 0^\circ$.

ial growth of atomic layers on surfaces. Finally, although Eq. (1) uses the single scattering expression, our results are quantitatively accurate for the 2 layer case at high energies (e.g., $E_k \geq 300$ eV). This is because in this work, we are only concerned with the intensity in a relatively narrow cone in the forward direction. For 3 or more layers, multiple scattering should further enhance the forward-direction focusing effect.

The authors wish to acknowledge valuable discussions with W. F. Egelhoff, Jr., B. Tonner, and S. Nagano. This work is supported by the National Science Foundation through Grant No. DMR-8405049 and Petroleum Research Fund Grant No. 1154-AC5,6.

*Visiting investigator, Synchrotron Radiation Center, University of Wisconsin, Madison, WI 53706.

¹W. F. Egelhoff, Jr., Phys. Rev. B **30**, 1052 (1984).

²H. C. Poon and S. Y. Tong (unpublished).

³C. H. Li, A. R. Lubinsky, and S. Y. Tong, Phys. Rev. B **17**, 3128

(1978).

⁴S. Kono, S. M. Goldberg, N. F. T. Hall, and C. S. Fadley, Phys. Rev. B **22**, 6085 (1980).

⁵Equations (1), (2), and this limiting result assume the plane-wave approximation.